Rooftop wind monitoring campaigns for small wind turbine applications: effect of sampling rate and averaging period

Amir Bashirzadeh Tabrizi[*a], Jonathan Whale[a], Thomas Lyons[b], Tania Urmee[a]

[a] *Physics and Energy Studies, School of Engineering and Information Technology, Murdoch University, Perth, WA 6150, Australia*

[b] *Environmental Science, School of Veterinary and Life Sciences, Murdoch University, Perth, WA 6150, Australia*

Abstract

Small wind turbines are often sited in more complex environments than the open terrain sites assumed in relevant installation guidelines or in the international small wind turbine design standard IEC61400-2. The built environment is an example of such a complex environment and installation of small wind turbines on the rooftops of high buildings has been suggested by architects and project developers as a potential means of incorporating sustainable energy generation into building design. In the absence of guidelines for installing wind turbines in the built environment, two key wind measurement parameters are the rate at which a data acquisition system (DAQ) samples the sensor, and the period over which the sampled data is averaged.

This paper presents the results of the effect of sampling rate and averaging period on turbulence measurements from a monitoring system on a building rooftop, in order to inform the process of developing guidelines. The results will inform the development of a Recommended Practice of wind resource assessment in the built environment, via the International Energy Agency Task 27. The key finding of the paper is that, in general, 10Hz sampling and 10 minutes averaging period give upper estimates for turbulence intensity and maximum values of the turbulence power spectra. Using these conservative values in the design of the turbine may be the best approach to ensure that the turbine can handle both the fatigue loads and resonance due to gusts.

Keywords: Small wind turbines, Built environment, Turbulence, Sampling rate, Averaging period.

Nomenclature

L	Monin- Obukhov length scale [m]
u_*	Friction velocity [m/s]

[*] Corresponding author. Tel.: +61893606713; e-mail: a.btabrizi@murdoch.edu.au. ; address: School of Engineering and Information Technology, Murdoch University, 90 South Street, Murdoch, WA 6150, Australia

$\overline{T_0}$	Mean air temperature [K]
g	Gravitational acceleration constant [m/s^2]
k	von Karmán constant [-]
$\overline{\acute{w}\acute{T}}$	Kinematic heat flux [mK/s]
σ_1	Standard deviation of longitudinal wind speed [m/s]
I_{15}	Characteristic turbulence intensity at 15 m/s [-]
a	Slope parameter for turbulence standard deviation model [-]
V_{hub}	Mean wind speed at the hub-height of the turbine [m/s]
$\vec{U}$	Wind velocity vector [m/s]
$\vec{\overline{U}}$	Mean wind velocity vector [m/s]
$\vec{\acute{U}}$	Fluctuation in the wind [m/s]
σ_x	Standard deviation of x [m^2/s^2]
z	Height of the anemometer a.g.l [m]
h	Height of the Bunnings warehouse façade a.g.l [m]
u_s	Longitudinal wind speed from the ultrasonic (raw data) [m/s]
v_s	Lateral wind speed from the ultrasonic (raw data) [m/s]
w_s	Vertical wind speed from the ultrasonic (raw data) [m/s]
u_{2d}	Longitudinal component of the horizontal wind speed [m/s]
θ	Wind direction in the horizontal plane [degree]
φ	Flow direction at an incline to the horizontal [degree]
$\sigma_{u_s v_s}$	Covariance between u_s and v_s [m^2/s^2]
$\sigma_{u_{2d} w_s}$	Covariance between u_{2d} and w_s [m^2/s^2]
u_{3d}	Longitudinal component of the three-dimensional wind speed (reference frame of the mean three-dimensional wind speed) [m/s]

v_{3d}	Lateral component of the three-dimensional wind speed (reference frame of the mean three-dimensional wind speed) [m/s]
w_{3d}	Vertical component of the three-dimensional wind speed (reference frame of the mean three-dimensional wind speed) [m/s]
I_u	Turbulence intensity for longitudinal wind component [-]
I_v	Turbulence intensity for lateral wind component [-]
I_w	Turbulence intensity for vertical wind component [-]

1. Introduction

The installation of small wind turbines (< 200 m^2 swept area [1]) on the rooftop of high buildings has been suggested by architects and project developers as a potential means of achieving a form of sustainable and low-energy buildings. Many rooftop installations, however, have suffered from poor siting [2,3] and have often bypassed a wind resource feasibility study prior to installation. As with all wind projects, large and small, a wind resource assessment is crucial in order to know the exact conditions that the wind turbine will experience.

For wind projects in open terrain, there exist a number of guidelines for conducting a monitoring campaign to assess the wind resource at the site [4,5]. The guidelines assume a clear distinction between the variations in wind speed due to large-scale macro-meteorological events and small-scale high frequency fluctuations. The mean wind speed is defined over an averaging period of 10 minutes in order to capture both. The IEC61400-12-1 standard provides a process for measuring the wind resource at a site and correlating with power measurements from a wind turbine situated close to the meteorological mast. For small wind turbines a period of 1 minute is chosen to accommodate the response of the small turbine to wind fluctuations. A site calibration may be carried out to account for differences between the measured wind speeds and turbine inflow conditions due to changes in the terrain around the site [5].

In both the US and UK, where significant markets for small wind turbines (SWTs) have been established [6,7] , the proportion of systems that are grid-connected is increasing whereas the proportion of systems off-grid is decreasing [8,9]. There is a also a growing trend for SWTs to be sited in more complex environments than the open terrain assumed in the aforementioned guidelines or in the international small wind turbine design standard IEC61400-2[10]. These sites include locations near buildings, trees and other obstacles. In such locations, the wind is normally highly three-dimensional, turbulent, unstable and light, in terms of direction and speed [11], and some sites may experience values of turbulence intensity that are many times greater than an open field site. Wind monitoring campaigns play a particularly important role for these turbulent sites since the level of turbulence significantly affects the power output of the turbine, and elevated turbulence intensity has been found to be the most important factor in reducing turbine fatigue life [12].

There are very few details in the literature on a methodology for conducting wind resource assessment campaigns in the built environment. In 2007, the Wind Energy Integration in Urban Europe (WINEUR) project released a report on resource assessment and recognised that, although expensive and time-consuming, there was no substitute for direct measurement in order to obtain quality data that will lead to accurate predictions of annual energy production [13]. As part of that project, direct measurements were conducted on rooftops of buildings in France and the UK. The monitoring methods were not specifically stated other than the use of cup anemometers and procedures that were similar to those for large-scale utility wind farms.

In the absence of guidelines, the monitoring methods for direct measurement of wind in urban areas have varied from study to study and in accordance with application. Two key measurement parameters are the rate at which a data acquisition system (DAQ) samples the wind sensor, and the period over which the sampled data is averaged. For instance, Anderson *et al.* sampled data at 10Hz and recorded as 10 minute averages on the rooftop of a three-storey building for the specific purpose of assessing the feasibility of the site for a small wind turbine installation [14]. On the other hand, Rotach used 1Hz data averaged over 50 minutes when measuring wind turbulence in urban street canyons as part of air pollution studies [15]. In designing a measurement campaign to capture the characteristics of the flow in the urban environment, consideration has to be given to (1) the choice of sensor, (2) whether the sampling rates are fast enough to accurately capture turbulence, and (3) whether the averaging period is suitably matched to the power spectra at the site.

Some literature is available on the comparison of different kinds of wind sensors for wind speed and turbulence characterization. Kristensen noted that the most significant error in mean wind speeds recorded by cup anemometers is due to lateral velocity fluctuations, and this error may be suppressed significantly by combining the cup anemometer with a wind vane and using a signal processing technique called the vector wind-run method [16]. Yahaya and Frangi compared measurements of turbulence using an ultrasonic anemometer and two opto-electronic cup anemometers and found that fast cup anemometers have the potential to measure some turbulence parameters (e.g. wind variance) with errors of magnitude as per those for mean speed measurements [17]. The U.S. Department of Energy's turbulence characterization program used propeller-vane and cup anemometers under very turbulent conditions, and the results suggested that the cup anemometer may prove to be an inexpensive and rugged sensor appropriate for turbulence measurements in wind energy applications [18]. On the other hand, Anderson *et al.* justify their use of an ultrasonic anemometer by stating that the output of cup anemometers is degraded at fast sample rates due to pulse counting demodulation, and in the highly dynamic and constantly changing wind environment of a rooftop, a significant amount of valuable data could be lost while the cup devices respond to change [14].

Researchers who are interested in accurately recording wind turbulence use a high frequency sampling rate, typically at or above 10 Hz [19]. If a spectral analysis of the high frequency turbulent regime is of interest, then a sampling rate related to the time constant of the measurement system is likely to be chosen (assuming this is sufficiently low) [20]. Lubitz studied the impact of ambient turbulence on the performance of a small wind turbine. Measurements recorded at 1 Hz showed a time lag of one to two seconds between a change in wind speed and the resulting change in energy production. [21].

The International Energy Agency (IEA) Task 27 was established in 2009 and is concerned with small wind turbine research [22]. The IEA Task 27 members have identified a need for a Recommended Practice on the micro-siting of small turbines in highly turbulent sites, such as the complex urban sites mentioned in this paper. The Recommended Practice will include best practice in site assessments in terms of a specific measurement and data acquisition strategy including sampling rate and averaging period analysis. Murdoch University is part of the IEA Task 27 working group and this paper presents the results of the effect of sampling rate and averaging period on turbulence measurements from a monitoring system on the rooftop of a building, in order to inform the process of developing the Recommended Practice. The specific objectives of this research are to:

(1) Investigate the effects of different sampling rates and averaging periods on the turbulent intensity and turbulence power spectra of the three components of wind flow (longitudinal, lateral and vertical) under the most common types of atmospheric conditions that a roof-mounted small wind turbine would operate in, and

(2) Compare the effect that sampling rate has on the value of the characteristic turbulence intensity, as defined in the international small wind turbine design standard, IEC61400-2, for small wind turbines mounted at different heights above a roof.

2. Theory

2.1. Turbulence Intensity

Turbulence is defined as "stochastic variations in wind velocity" from mean values in three dimensions; longitudinally, laterally and vertically. In wind resource analysis, one measure of turbulence is given by the dimensionless quantity, turbulence intensity, *I*, which is the ratio of the wind speed standard deviation to the mean wind speed, measured from the same set of data [1]. The intensity of turbulence has been studied via various field and wind tunnel experiments in and above canopies. Measurements of standard deviations of velocity component fluctuations show that these variables are very scattered within canopies. The scatter is due to the effects of pressure gradients as well as the structure of the canopy and turbulence characteristics above the canopy [23].

The small wind turbine standard IEC6400-2: Design requirements for small wind turbines (ed. 2) uses a Normal Turbulence Model (NTM) that describes turbulence and turbulence intensity and includes the effects of varying wind speed and varying direction [1]. IEC6400-2 defines a 'characteristic turbulence intensity', as the 90^{th} percentile of turbulence intensity measurements binned with respect to wind speed [1]. For each wind speed bin, the 90^{th} percentile value of *I* is obtained by taking the mean *I* value in the bin plus 1.28 standard deviations of *I* from the mean, thus assuming a Gaussian distribution for turbulence intensity values. The Normal Turbulence Model (NTM) states that the expected standard deviation of longitudinal wind speed, σ_1, is given by following equation [1] based on data collected from open terrain sites:

$$\sigma_{1(90\%)} = I_{15}(15 + aV_{hub}) / (a + 1) \qquad (1)$$

The necessary minimum requirements of the NTM in terms of load analysis of regular wind turbines is discussed by Stork *et al.* , who state that the curve for σ versus V_{hub} is based on observations of hub-height wind speeds in the range 10-25 m/s over open terrain [24].

2.2. Turbulence and Thermal Stability

A three-dimensional wind velocity vector $\vec{U}$ can be defined as

$$\vec{U} = \vec{\overline{U}} + \vec{\acute{U}} \qquad (2)$$

The term 'spectra' is applied to describe the functions of frequency and the function that presents turbulence as a function of frequency is recognized as a 'spectral density' function [25, 26].
Turbulence is affected by the atmospheric thermal stability conditions, which depend on the potential temperature gradient. In unstable conditions, the temperature gradient is negative and the air near to the ground is warmer with a lower density than the surrounding air, resulting in positive buoyancy forces that move a parcel of air upwards. The turbulent eddies in an unstable boundary layer can extend vertically for a significant distance. In a neutral, or near neutral atmospheric condition, the air is well-mixed and the vertical potential temperature gradient is close to zero, resulting in buoyancy forces that are close to zero. High wind speeds and cloudy skies prevent any significant temperature gradient and lead to neutral atmospheric conditions [27].

The cut-in wind speed for most small wind turbines that are appropriate for rooftop applications is, at a very minimum, 2 m/s and most of the power generated by a turbine on the roof occurs at wind speeds greater than 4 m/s. For most operating conditions of small rooftop wind turbines, the atmospheric stability is either slightly unstable or neutral [28].

The atmospheric boundary layer can be specified according to the parameter known as the Monin-Obukhov length, *L*; which is the height where the turbulent forcing from thermal and shear processes are in balance. *L* is constant with height but changes with stability in the surface layer and as a result can be used as a stability parameter [29]. *L* is defined as:

$$L = \frac{-u_*^3 \overline{T_0}}{g\kappa \overline{\acute{w}\acute{T}}} \qquad (3)$$

Golder, using micro-meteorological data, calculated *L* (the Monin-Obukhov length) values and Pasquill atmospheric stability classes and obtained curves presenting atmospheric stability classes as functions of *L* and roughness length, z_0 [30]. This curve can be used to select wind data with respect to a range of Monin-Obukhov lengths to choose data that correspond to particular atmospheric stability conditions.

It should be noted that the Monin-Obukhov analysis was originally proposed as a stability correction to the logarithmic law for the mean wind speed profile which is normally modelled as a fully developed wind profile over homogeneous and uniformly rough terrain under

steady state conditions. Such a situation is never going to be appropriate to urban flows but Rotach [31] suggests that when the wind speeds and temperatures are averaged over all wind directions, their gradients can be described using MO theory based on local values of the scaling parameters. Since sensible heat flux was not measured the analysis of Golder has been used to estimate the Monin-Obukhov length scale to classify atmospheric stability.

3. Method

3.1 Site Measurements

This study makes use of data collected from a wind monitoring system on the roof of a large warehouse belonging to the hardware chain Bunnings Ltd. in the suburb of Port Kennedy, Perth, Western Australia. The warehouse is a rectangular building, with its long-axis oriented NNE-SSW, a façade wall that extends above the roof and is h = 8.5 m a.g.l, and a very low pitched roof (almost flat). The building lies approximately 5km distant from the coast (Indian Ocean) with the prevailing winds from the south-west. The warehouse is situated in a commercial estate but has no larger buildings or large trees in the vicinity. Within a 1km radius of the site there are mainly residential buildings to the north, commercial and industrial buildings to the east and a few buildings, low shrubs and low sand dunes to the south and west. The south-west front and the north-west side are comparatively open, though street furniture [1] and a car park exist on these sides [32]. The built-up area surrounding the warehouse is shown in Figure 1.

The wind monitoring system was installed in September 2009 as part of a wind resource assessment for the installation of five small wind turbines that were later commissioned in March 2010. A Gill WindMaster Pro 3D ultrasonic anemometer was installed on a boom on a 5.3 m mast attached to the front-façade of the warehouse. The boom had a sliding collar in order to position the ultrasonic anemometer at different heights above the roof. The mast could be tilted down in order to make adjustments or to replace sensors. The data consists of 10Hz data over a 2 year period. To reduce processing time, smaller records of 10 days of data were extracted for each of 4 normalized heights studied; z/h = 1.35, 1.46, 1.58 and 1.70, where z is the height of the anemometer a.g.l. The choice of 10 days of measured wind data was driven by a need to provide a balance between having enough data that would capture changes in average wind speed from events that typically occur over several days whilst avoiding the collection of too much data, particularly at high sampling rates, which adds complexity in terms of data storage, transfer and analysis. . In this paper, the results for mean turbulence intensity and power spectral density are presented for z/h = 1.46, which is a representative height for small wind turbines on the roof. The results for all 4 heights, however, are included in the study of characteristic turbulence intensity. Figure 2 indicates the position of the ultrasonic anemometer on the roof.

[1] Objects and pieces of equipment installed on streets and roads for various purposes

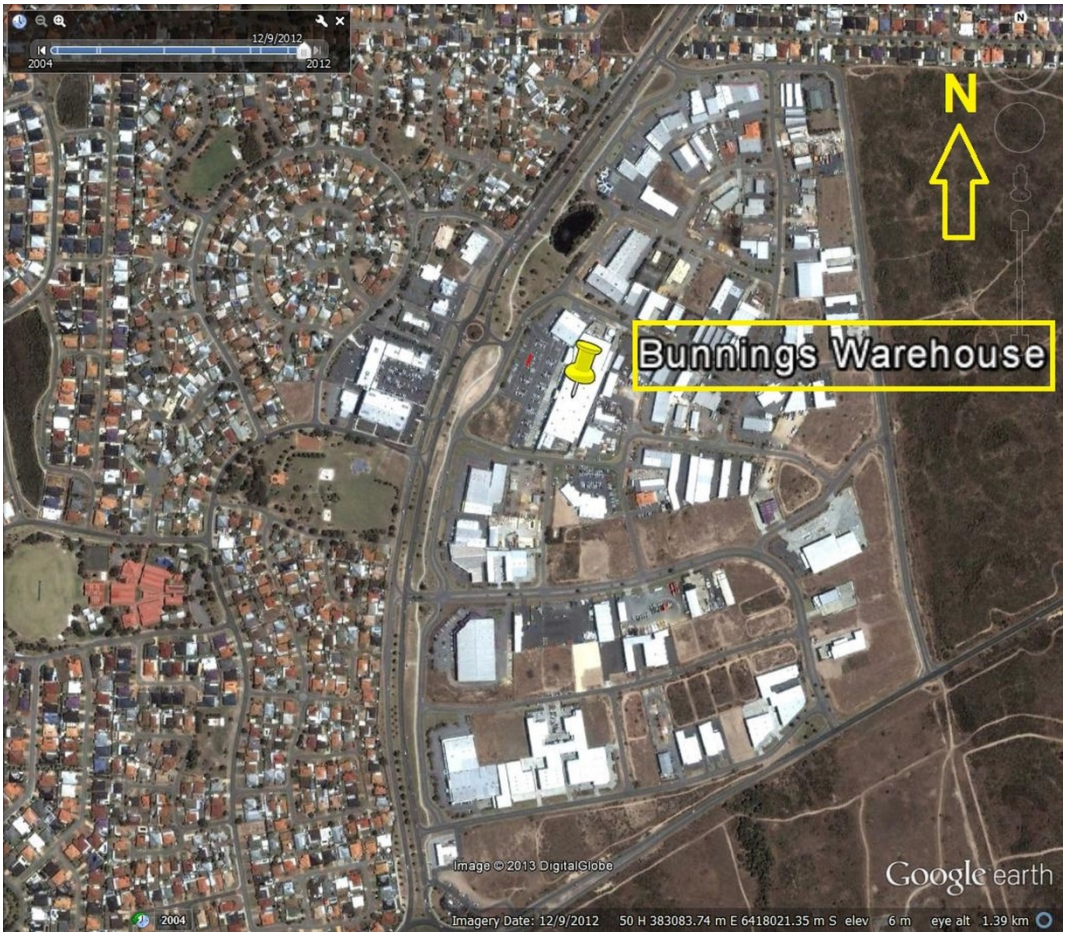

Figure1. Aerial view of the built-up area surrounding the Bunnings warehouse in Port Kennedy, WA.

Figure 2. A photograph of the front view of the Bunnings warehouse showing the five small wind turbines and the ultrasonic anemometer position (red circle).

3.2. Data Processing

The data series of 10 days of 10 Hz measured data from the rooftop of the warehouse were filtered to produce a number of datasets with lower sampling rates, in order to compare turbulence characteristics between datasets. In addition the original 10Hz dataset was analysed to see the effect of different averaging periods on turbulence characteristics.

As stated in Section 2, the most common atmospheric conditions experienced during the operation of a small wind turbine in the built environment are either slightly unstable or neutral atmospheric conditions. Based on a table of roughness length, surface characteristics and roughness class from the European wind atlas, the aerodynamic roughness of Bunnings warehouse area was estimated to be 50 cm [33]. The curves presented by Golder were then used to find the range of Monin-Obukhov lengths corresponding to slightly unstable and neutral condition on the roof of the warehouse for 10 minutes averaging period and these values were used to filter the raw measurements [30].

The next part of the procedure was to change from the ultrasonic anemometer reference frame to the reference frame of mean three-dimensional wind speed (longitudinal, lateral and vertical) and direction. This allowed the measured data to be compared to the values from the NTM model in IEC61400-2. The filtered data for each dataset was binned with respect to different time periods and averages, allowing standard deviations of data for each bin to be calculated. As a first step, the time-averaged data was used to compute the wind direction in the horizontal plane, θ, along with the covariance, $\sigma_{u_s v_s}$. These parameters were used to translate the data from the reference frame of the ultrasonic anemometer to the reference frame of the horizontal wind speed and direction, in accordance with:

$$\sigma_{u_{2d}}^2 = \sigma_{u_s}^2 \,.\cos^2\theta + \sigma_{v_s}^2 \sin^2\theta - 2\sin\theta\cos\theta\,.\sigma_{u_s v_s} \quad (4)$$

$$\sigma_{v_{2d}}^2 = \sigma_{v_{3d}}^2 = \sigma_{u_s}^2 \,.\sin^2\theta + \sigma_{v_s}^2\,.\cos^2\theta + 2\sin\theta\cos\theta\,.\sigma_{u_s v_s} \quad (5)$$

Figure 3a shows the first step in changing referencing frame. In the next step, averages and standard deviations of u_{2d} and w_s in each bin were calculated. From the time-averaged data the direction of flow at an incline to the horizontal, φ, was computed along with the covariance $\sigma_{u_{2d} w_s}$. In a process similar to the first step, these parameters were used to translate the data from the reference frame of the horizontal wind speed to the reference frame of the mean three-dimensional wind speed and direction, in accordance with :

$$\sigma_{u_{3d}}^2 = \sigma_{u_{2d}}^2 \,.\cos^2\varphi + \sigma_{w_s}^2 \sin^2\varphi + 2\sin\varphi\cos\varphi\,.\sigma_{u_{2d} w_s} \quad (6)$$

$$\sigma_{w_{3d}}^2 = \sigma_{u_{2d}}^2 \,.\sin^2\varphi + \sigma_{w_s}^2\,.\cos^2\varphi - 2\sin\varphi\cos\varphi\,.\sigma_{u_{2d} w_s} \quad (7)$$

Figure 3b shows the second step in changing referencing frame. The turbulence intensity for each wind component was then calculated according to:

$$I_u = \sqrt{\sigma_{u_{3d}}^2}/\bar{U}, I_v = \sqrt{\sigma_{v_{3d}}^2}/\bar{U}, I_w = \sqrt{\sigma_{w_{3d}}^2}/\bar{U} \quad (8)$$

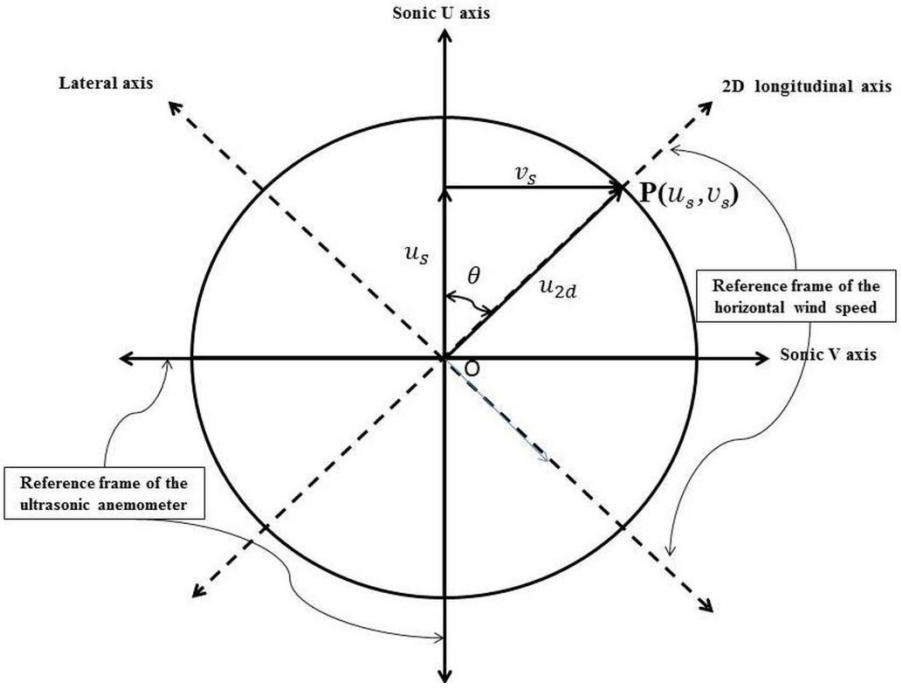

Figure 3a. Changing the reference frame of the ultrasonic anemometer to the reference frame of the horizontal wind speed.

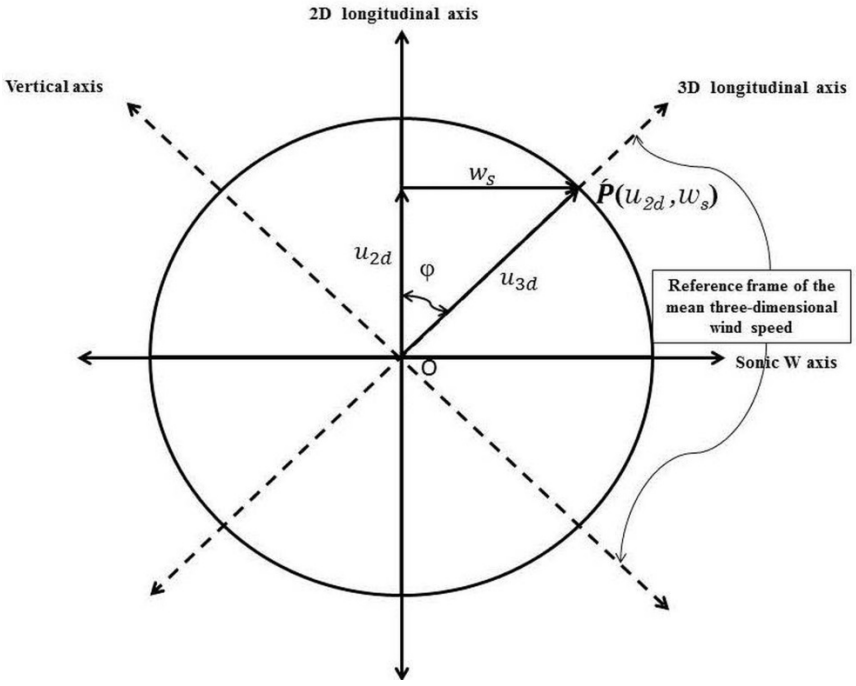

Figure 3b. Changing the reference frame of the horizontal wind speed to the reference frame of the mean three-dimensional wind speed.

To investigate the effect of sampling rate on the turbulent wind regime experienced by small wind turbines in the built environment, the above procedure for calculating turbulence intensity was performed on three datasets with different sampling rates; 1Hz, 4Hz and 10Hz, with an averaging period of 10 minutes (the standard averaging period used in wind monitoring studies). The rationale for choosing these sampling frequencies was largely based on previous studies concerned with the effect of turbulence on small wind turbines. Lubitz used 1Hz data based on the time lag in the response of the small wind turbine energy production to changes in wind speed [21]. SWT manufacturer Quiet Revolution and the Energy Savings Trust studies used 4Hz with all their rooftop installations. Anderson et al. used 10Hz and this has been used by others looking at turbulence in detail e.g. [14].

To investigate the effect of averaging period on turbulence the above procedure for calculating turbulence intensity was performed on the 10 Hz data using three different averaging periods; 10 minutes, 5 minutes and 1 minute. The rationale for choosing these averaging periods was based on values used from previous studies. The UK body SWIIS has recommended a 10-minute sampling standard for measuring turbulence [34]; the Warwick Wind Trial data analysis suggests 5-minute averaging may be more representative in urban areas [35]; other groups have used 1-minute averaging in accordance with the procedures of power performance measurement of small wind turbines in IEC61400-2 Annex H [1].

For the different sampling rates and averaging periods noted above, the value of the characteristic turbulence intensity, I_{15} has been calculated by using a linear fit to the scatter plot of standard deviation versus mean of the longitudinal wind speed, extrapolating the fit and substituting 15 m/s as the mean wind speed. The results are compared with the values from the NTM of IEC61400-2, which were generated using Eq. 1.

To find the power spectral density for each dataset the mean longitudinal, lateral and vertical wind components are separately subtracted from their respective measurements to leave the fluctuations for each component. The normalized autocorrelation of the fluctuations is then computed and a Fast Fourier Transform of this autocorrelation provides the data for the power spectral density plots. To investigate the effect of sampling rate on turbulence power spectral density, the data in neutral atmospheric conditions (243 records, each of ten minutes duration and taken at z/h = 1.46) were sampled at 1Hz, 4Hz and 10Hz, respectively, to produce the power spectra presented here.

To investigate the effect of averaging period on turbulence power spectral density data set sampled at 10 Hz at z/h = 1.46 above the roof façade in neutral atmospheric conditions were used. During 10 days of measured wind data, there were 243 groups of ten-minute readings taken in neutral atmospheric conditions. This same data was divided into 468 groups of five-minute reading as well as 2430 groups of one-minute readings. The different groupings of the same dataset were then used to investigate the effect of averaging period on turbulence power spectral density.

This approach uses the highest possible sampling rate from the experiment (10Hz) when investigating the impact of averaging period on time-averaged turbulence intensity. This couples the requirement for sufficient number of samples to ensure convergence of turbulence intensity with the frequency needed to provide adequate resolution of spectra. Although there is evidence that the spectral gap [36] may not exist at some sites [37], our data suggest a convergence of results beyond a 10 minute averaging period consistent with the

presence of a spectral gap. Since the sampling rate determines the spectra and the spectral gap influences the choice of averaging period, there is thus an interdependency of sampling rate and averaging period which makes it difficult to exactly determine the individual effect of either parameter on time-averaged turbulence intensity. This must be noted as a limitation of the research.

4. Results and Discussion

4.1. Turbulence Intensity

Figures 4, 5 and 6 show the mean of turbulence intensity for longitudinal, lateral and vertical wind components, respectively. Each figure shows the effect of three different sampling rates on 10 minute averaged data collected at z/h = 1.46 for slightly unstable and neutral conditions. Note that the error bars in Figures 4, 5 and 6 represent the standard deviation of binned turbulence intensity values and the number of measured data points in each bin for the 10 Hz case is displayed in brackets on the plots. Due to the low number of measured neutral condition data for last bin, this bin has not been included in the analysis.

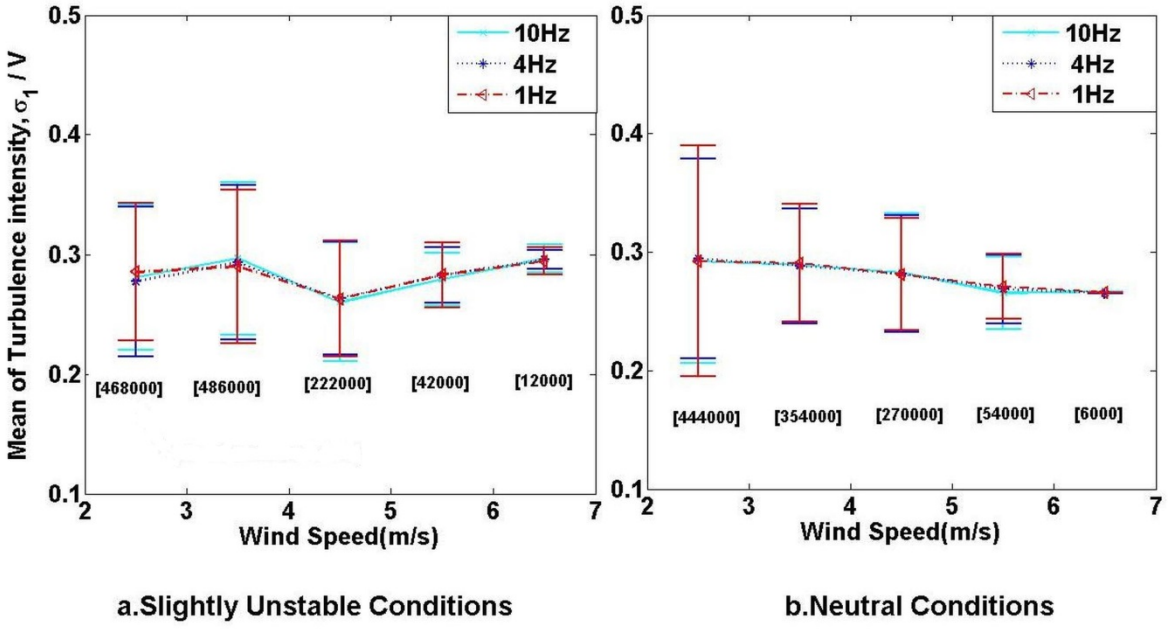

Figure 4. Effect of different sampling rates on mean of turbulence intensity (longitudinal component), z/h = 1.46 (the values in the brackets show the numbers of measured data).

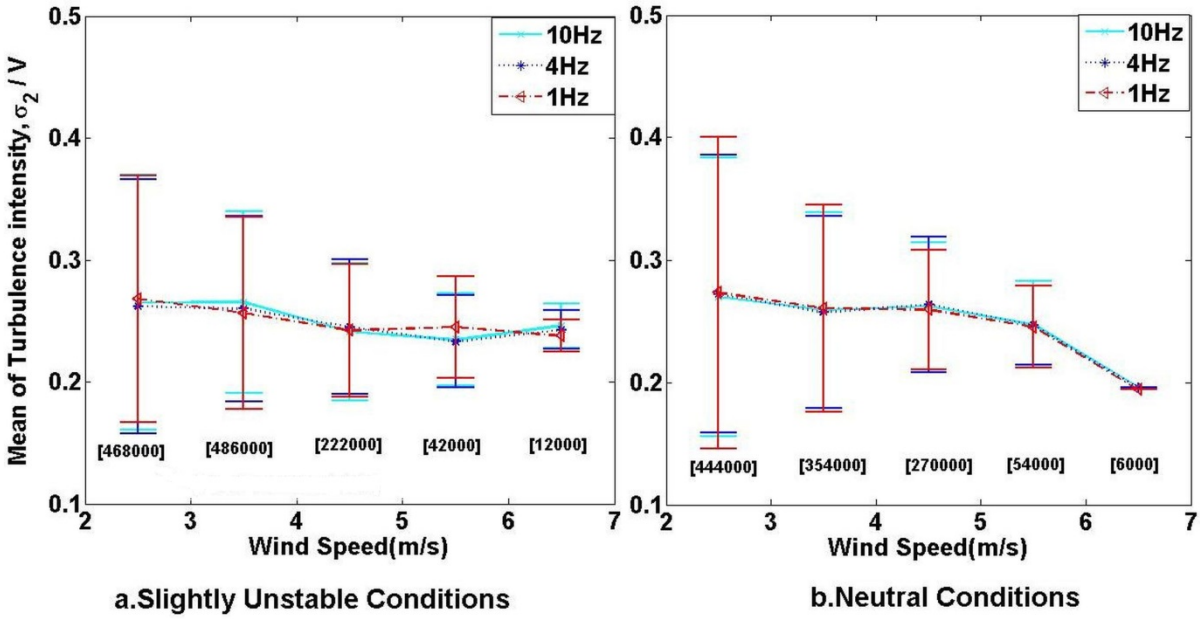

Figure 5. Effect of different sampling rates on mean of turbulence intensity (lateral component), *z/h* = 1.46(the values in the brackets show the numbers of measured data).

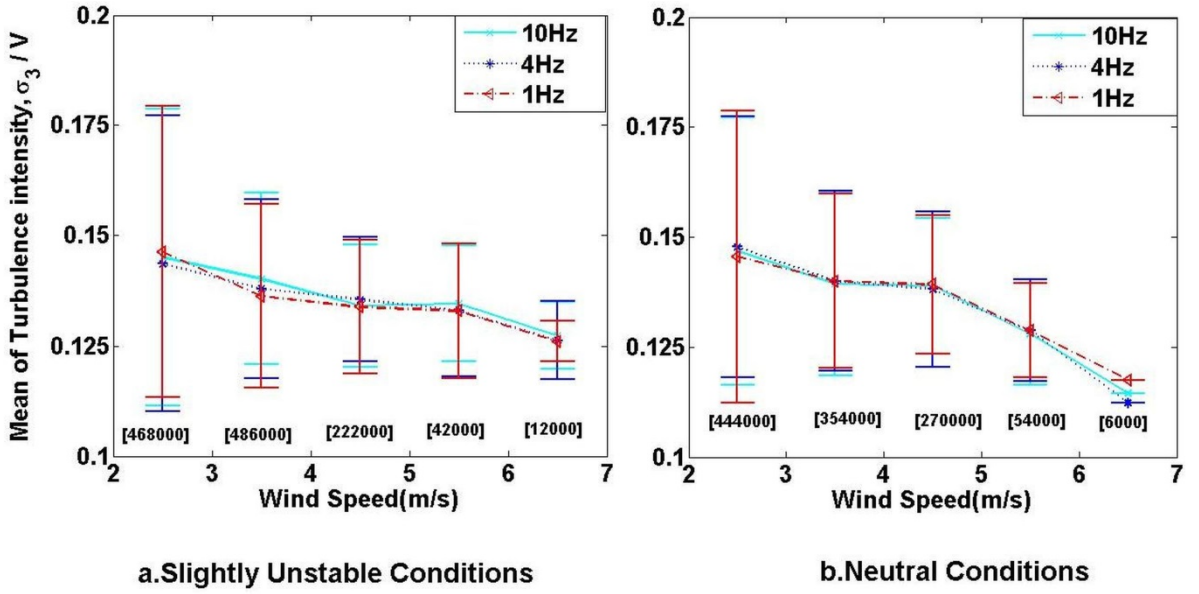

Figure 6. Effect of different sampling rates on mean of turbulence intensity (vertical component), *z/h* = 1.46(the values in the brackets show the numbers of measured data).

Figures 4, 5 and 6 are striking in that there are only slight differences in mean turbulence intensity for the three wind components with respect to the three different sampling rates. To quantify this, for slightly unstable conditions, the maximum relative percentage difference between mean turbulence intensity values from the 10 Hz and 1 Hz data sets is 2.23%, 4.34% and 2.79% for the longitudinal, lateral and vertical components, respectively, and for neutral conditions these values reduce to 2.05%, 1.36% and 0.89%. Generally, in neutral atmospheric conditions the calculated values for mean turbulence intensity of all wind components are less sensitive to sampling rate compared to slightly unstable conditions. This discrepancy may be due to buoyancy effects because of the differential heating of buildings under slightly unstable conditions. These results clearly show that there is no significant

difference between the results of the different sampling rate study in terms of turbulence intensity.

Where there is good agreement in mean turbulence intensity values across the range of sampling frequencies, the standard deviation of turbulence intensity is greatest for the lowest sampling rate. This is particularly evident at low wind speeds and in consistent with the results of Hristov [13]. For slightly unstable conditions, the maximum relative percentage difference between the standard deviation of turbulence for the 10 Hz and 1 Hz data sets is 24.98%, 9.57% and 16.07% for the longitudinal, lateral and vertical components, respectively, while for neutral conditions these values reduced to 12.98%, 11.51% and 8.72%.

Figures 7, 8 and 9 show the mean of turbulence intensity for longitudinal, lateral and vertical wind components, respectively. Each figure shows the effect of three different averaging periods on data sampled at 10 Hz measured at z/h = 1.46 in both slightly unstable and neutral conditions.

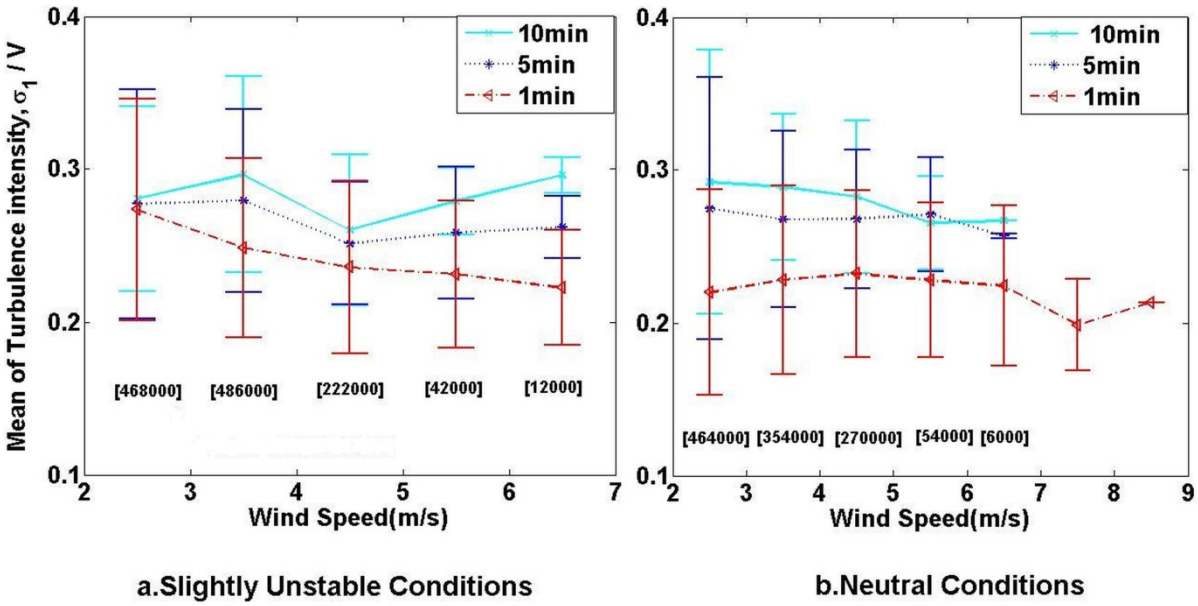

Figure 7.Effect of different averaging time on mean of turbulence intensity (longitudinal component), z/h = 1.46(the values in the brackets show the numbers of measured data).

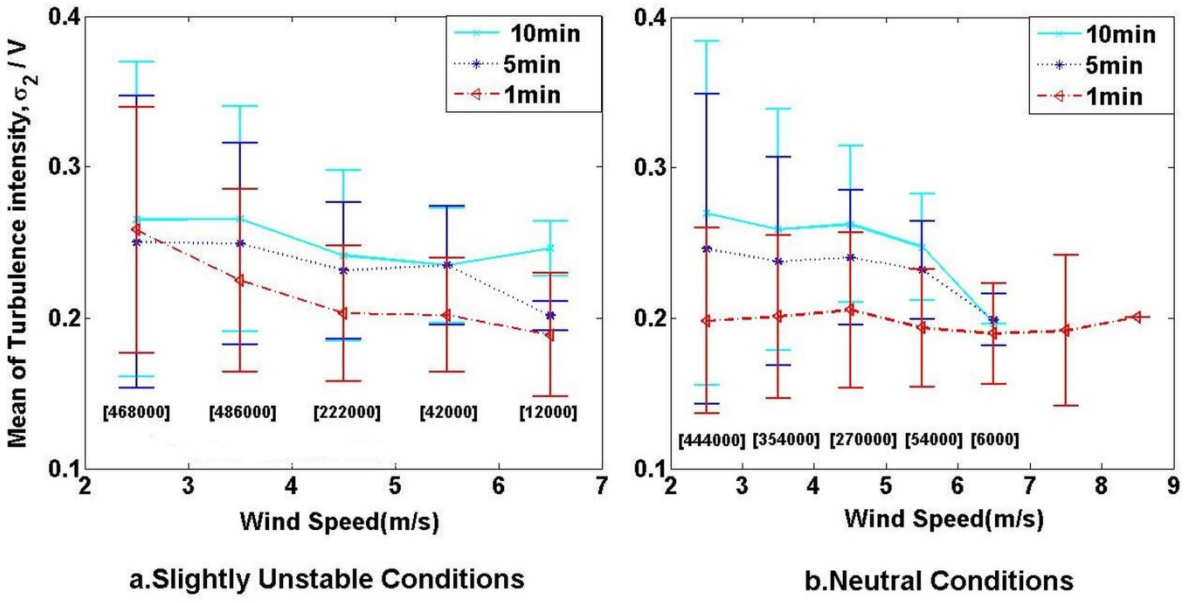

Figure 8.Effect of different averaging time on mean of turbulence intensity (lateral component), *z/h* = 1.46(the values in the brackets show the numbers of measured data).

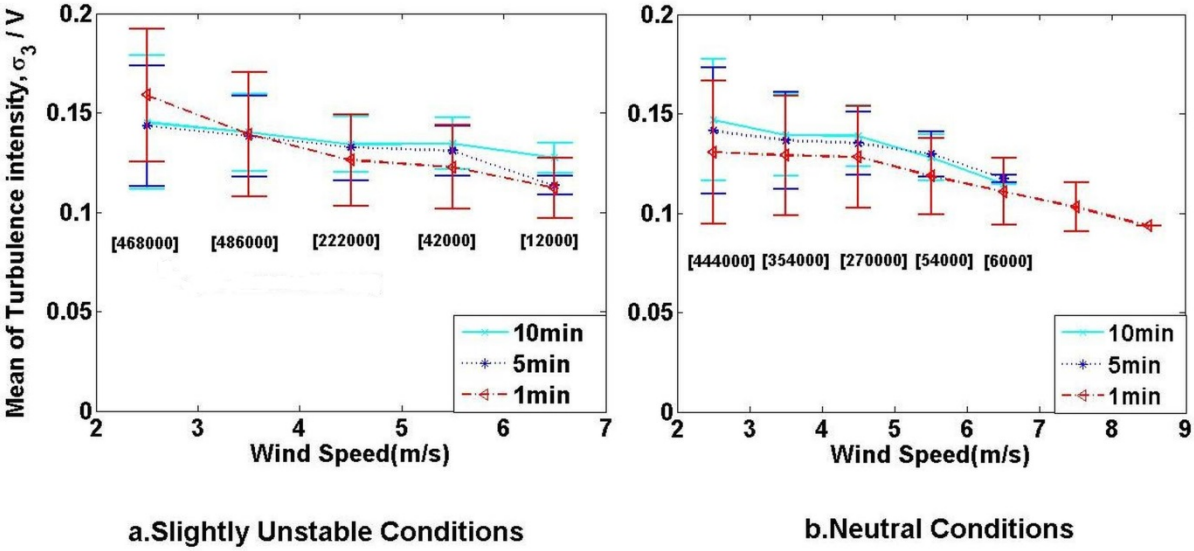

Figure 9.Effect of different averaging time on mean of turbulence intensity (vertical component), *z/h* = 1.46(the values in the brackets show the numbers of measured data).

The results show that the vertical component of mean turbulence intensity was much less sensitive to changes in averaging period than either the longitudinal or lateral components. To quantify this, for neutral conditions, the maximum relative percentage difference between the values of the vertical component of turbulence intensity in Figure 9, comparing 10 minute and 1 minute averaging periods, is 11.01% (neutral conditions) and 9.43% (slightly unstable conditions). In contrast, the longitudinal and lateral components of turbulence intensity were significantly more sensitive to averaging period than the vertical component and this could be a function of the horizontal scale of the local environment; in general, for both atmospheric conditions, decreasing averaging period decreases the value of calculated turbulence intensity. As an example, the maximum relative percentage difference between the values of

the lateral component of turbulence intensity in Figure 8(b), reduced from 27% to 20% by shortening the averaging period from 10 minutes to 1 minute in neutral conditions. Similarly for slightly unstable conditions, the maximum relative percentage difference between the values of the longitudinal component of turbulence intensity in Figure 7(a) decreases from 29% to 22% by reducing the averaging period from 10 minutes to 1 minute. Again, the number of measured data points in each bin for the 10 Hz case is shown in brackets in Figures 7, 8 and 9. Due to the low number of measured neutral conditions data for last two bins, the numbers of points have not been displayed and the data in these last bins has not been included in the analysis.

It is likely that the lower values of mean turbulence intensity when using shorter averaging periods is due to the fact that a longer time period has a greater probability of capturing a greater range of wind conditions and hence a greater deviation of wind speeds. The figures clearly show that a 10 minute averaging period gives the largest TI and suggests that monitoring with a 1 minute or 5 minute averaging period will not provide accurate enough results. On the other hand, it should be noted that 5 minute or 10 minute averages can always be calculated from 1 minute averages but not the other way around.

Table 1 provides the calculated values of characteristic turbulence intensity I_{15} for different heights above the roof and different sampling rate. Figure 10 shows an example of how measured mean and standard deviation of wind speed data, in this case at z/h = 1.70, are used to estimate I_{15} using extrapolation of a linear fit.

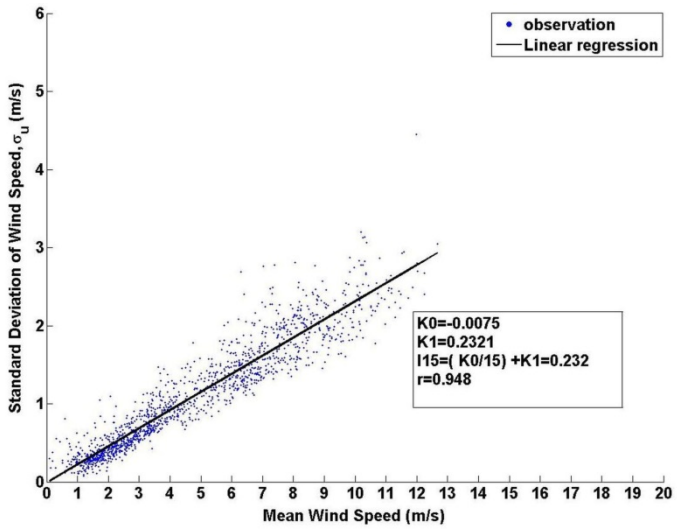

Figure 10. Estimation of characteristic turbulence intensity I_{15} using extrapolation of a linear fit to measured standard deviation versus mean wind speed data (longitudinal component), z/h = 1.70 using a 10Hz sampling rate and a 10 minute averaging period.

Table 1
Calculated values of I_{15} for different heights above roof and different sampling rates (10 minute averaging period)

Normalized Height	Sampling Rate(Hz)	I_{15}	Correlation Coefficient
	1	0.241	0.817
1.35	4	0.241	0.818
	10	0.241	0.818
	1	0.282	0.883
1.46	4	0.282	0.883
	10	0.282	0.883
	1	0.252	0.925
1.58	4	0.251	0.924
	10	0.251	0.924
	1	0.232	0.947
1.70	4	0.232	0.948
	10	0.232	0.948

Comparing the calculated I_{15} values at each height with respect to sampling rate, it is clear that the estimated value of I_{15} has not been significantly affected by sampling rate; for all heights studied, a change in sampling rate from 1 Hz to 10 Hz resulted in less than 0.15% change in the value of $I_{15.}$

Table 2 provides the calculated values of I_{15} for different heights above roof and different averaging periods.

Table 2
Calculated values of I_{15} for different heights above roof and different averaging periods (10 Hz sampling rate)

Normalized Height	Averaging Period (min)	I_{15}	Correlation Coefficient
	1	0.199	0.756
1.35	5	0.234	0.812
	10	0.241	0.812
	1	0.236	0.862
1.46	5	0.275	0.884
	10	0.282	0.883
	1	0.208	0.894
1.58	5	0.242	0.929
	10	0.251	0.924
	1	0.192	0.912
1.70	5	0.222	0.944
	10	0.232	0.948

Comparison of the calculated I_{15} values in Table 2 clearly shows that the averaging period has a significant effect on the value of I_{15}, and reducing the averaging period results in lower values of I_{15}. As example, for z/h = 1.70 reducing the averaging period from 10 minutes to 1 minute decreases the value of I_{15} by 17% and at z/h = 1.46, shortening the averaging period

causes a 16% reduction for I_{15} . It is notable that the difference between the calculated values of I_{15} according to 10 minutes averaging period and 5 minutes averaging period is so close.

The value of I_{15} was observed to increase with height to achieve its maximum at z/h = 1.46 and thereafter decreased with height. Although these measurements for different elevations were not taken at the same time, the location of the maximum longitudinal variance is consistent with the result that Rotach achieved through simultaneous measurement at different elevations (between z/h =1.4 and z/h =1.6) [9]. Also measuring at higher heights moves the sensor out of the building turbulence wake and there is less scatter in the data leading to higher correlation coefficients.

The calculated value for I_{15} at rooftop in built environment for all cases is significantly higher than the I_{15} based on the IEC6400-2 standard (18%); this questions the use of I_{15} as characteristic standard turbulence intensity for small wind turbine applications in built-environment. Equation 1 of this paper (taken from the IEC6400-2 standard) is based on open terrain data with wind speeds in the range 10-25 m/s [18], yet such speeds are unlikely to be experienced in urban applications. It also implicitly assumes that wind speeds have a Gaussian distribution and while Panofsy and Dutton [38] have shown this to be appropriate for open terrain applications, such an assumption is questionable within the complex urban environment [39]. Thus I_{15} as a measure of the characteristic turbulence intensity for small wind turbine applications in built-environment is inappropriate and a lower characteristic intensity i.e., I_5 or $I_{10;}$ should be investigated as an alternative metric for the characteristic turbulence intensity for urban wind regimes. In addition, a brief inspection of the turbulence intensity for the 10Hz dataset indicates non-Gaussian behaviour, particularly in low wind speeds and further research is required to investigate the probability distribution of turbulence intensity data.

4.2. Turbulence Power Spectra

The turbulent wind spectra for an average of 243 records at a representative height (z/h = 1.46) in neutral atmospheric conditions and three different sampling rates are shown in Figure 11 for the longitudinal, lateral and vertical components of turbulent wind fluctuations.

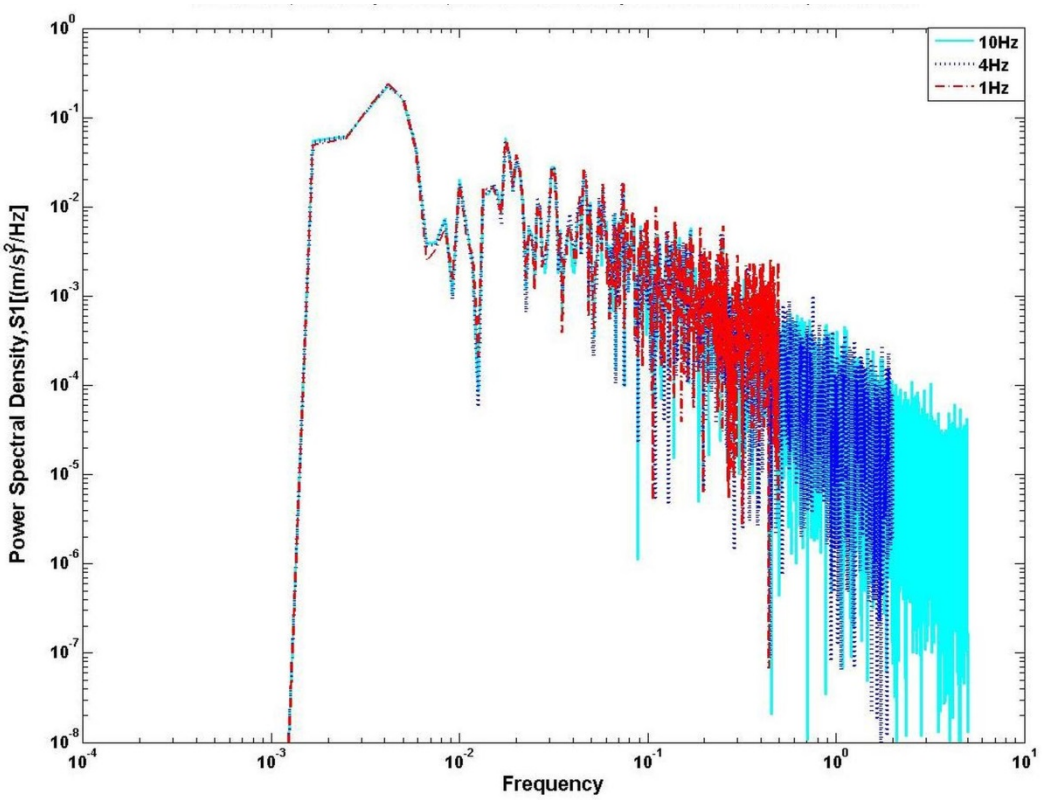

Figure 11a.Effect of different sampling rates on the power spectral density of the longitudinal component of turbulent wind fluctuations, *z/h* = 1.46 in neutral atmospheric conditions.

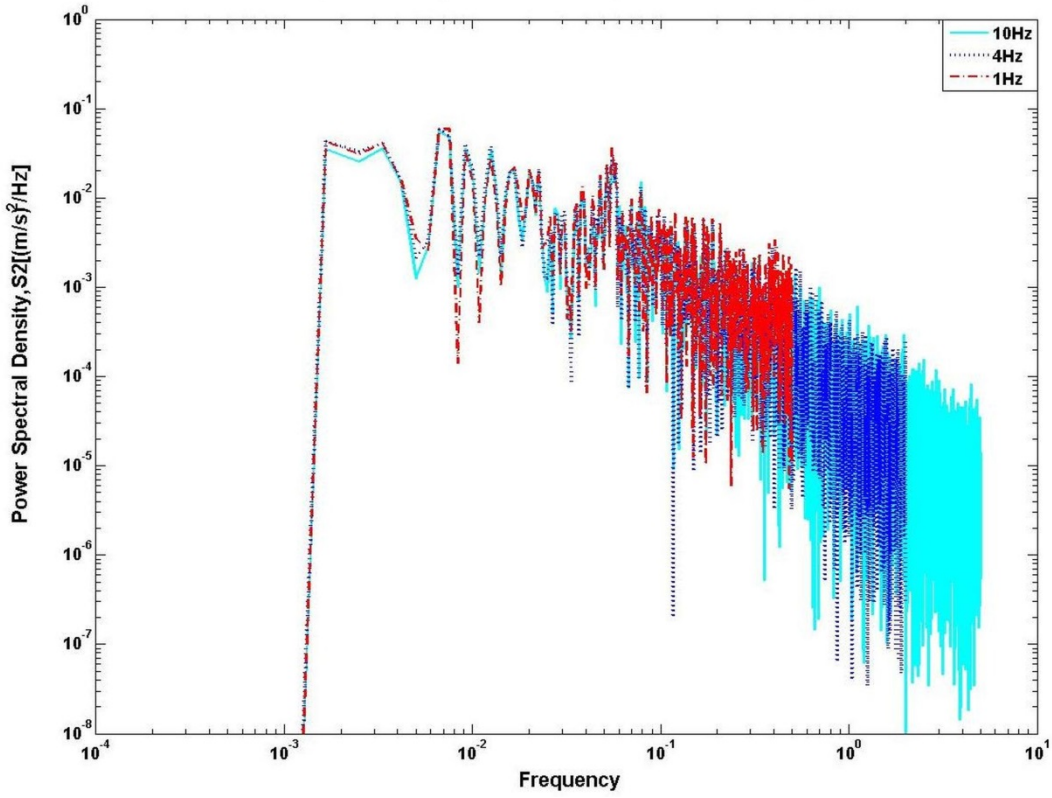

Figure 11b. Effect of different sampling rates on the power spectral density of the lateral component of turbulent wind fluctuations, *z/h* = 1.46 in neutral atmospheric conditions.

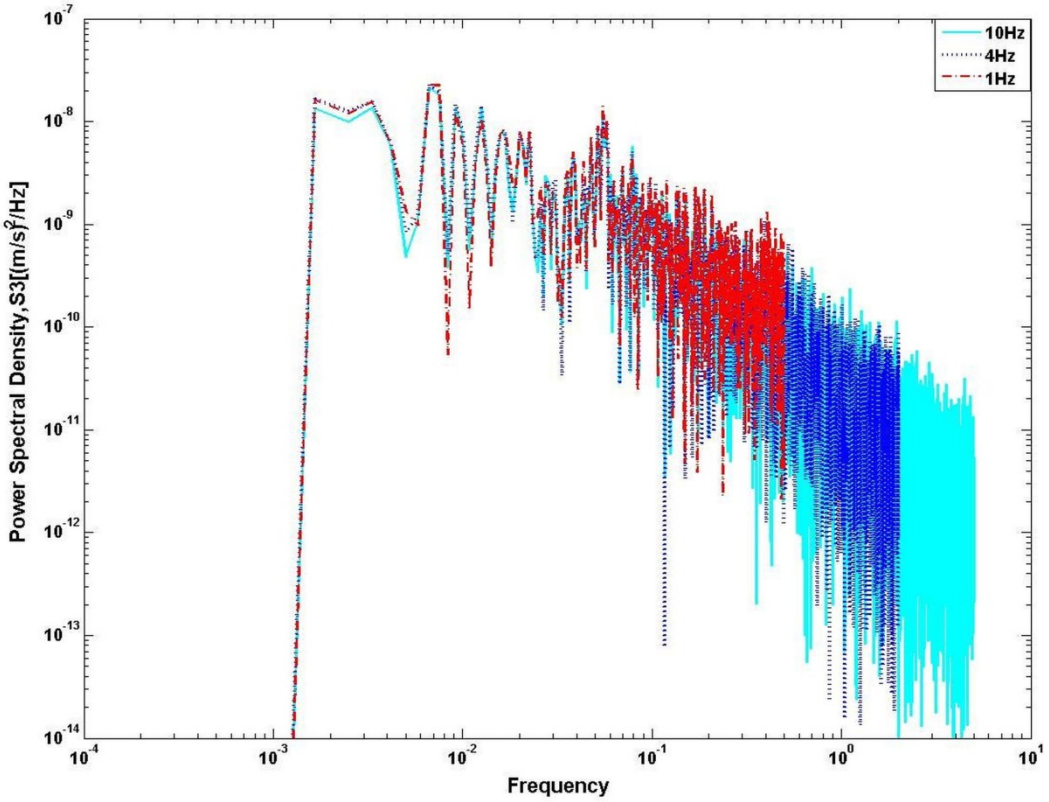

Figure 11c. Effect of different sampling rates on the power spectral density of the vertical component of turbulent wind fluctuations, z/h = 1.46 in neutral atmospheric conditions.

Figure 11 shows that for all three turbulent wind components, the values of power spectral density are not very sensitive to different sampling rates and the maximum value of the spectra for the three different sampling rates are very similar. The trends of the spectral density curves for different sampling rates are, for each wind component, almost coincident but it is clear that the spectrum covers a greater frequency range for higher sampling rates, as expected. For all sampling rates maximum peaks are observed around 0.01 Hz for longitudinal, lateral and vertical components;

The turbulent wind spectra at a representative height (z/h = 1.46) for an average of 243, 486 and 2430 records for three different averaging periods (10 minutes, 5 minutes and 1 minute) in neutral atmospheric conditions are shown in Figure 12 for the longitudinal, lateral and vertical components of turbulent wind fluctuations.

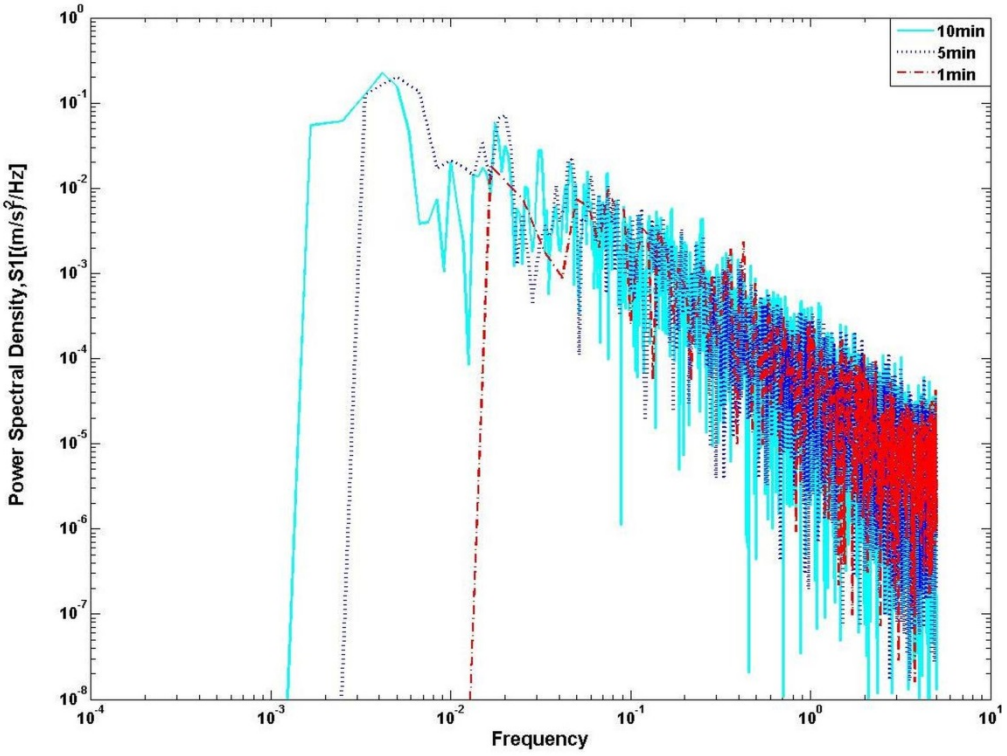

Figure 12a. Effect of different averaging periods on the power spectral density of the longitudinal component of turbulent wind fluctuations, z/h = 1.46 in neutral atmospheric conditions.

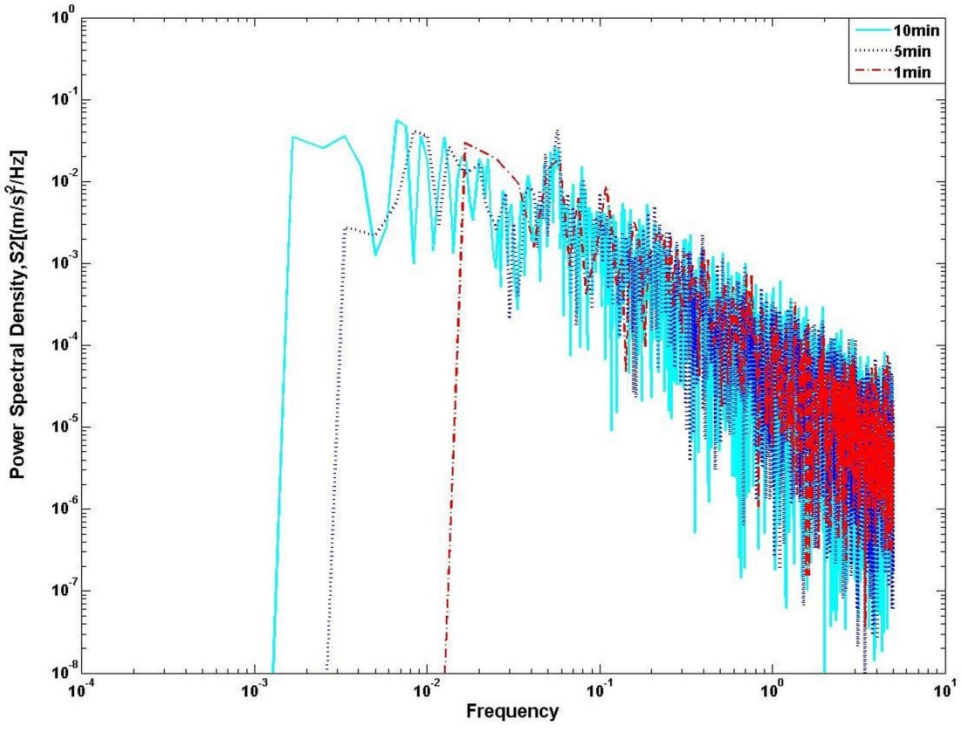

Figure 12b. Effect of different averaging periods on the power spectral density of the lateral component of turbulent wind fluctuations, z/h = 1.46 in neutral atmospheric conditions.

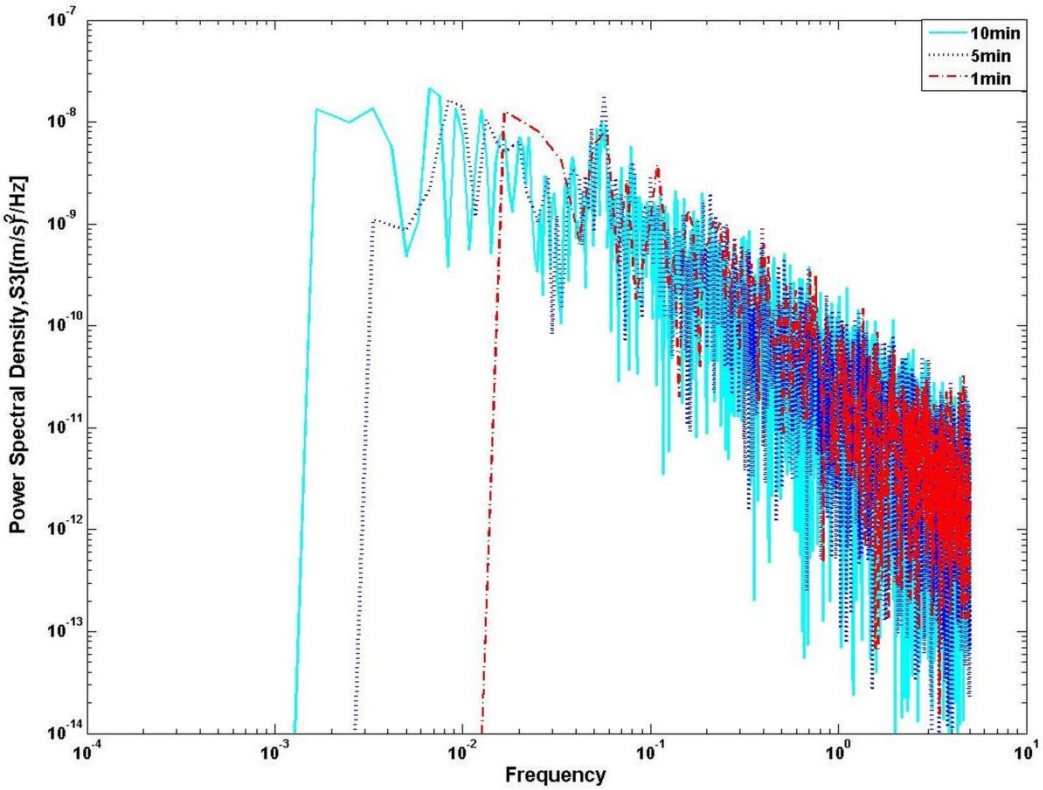

Figure 12c. Effect of different averaging periods on the power spectral density of the vertical component of turbulent wind fluctuations, z/h = 1.46 in neutral atmospheric conditions.

The results show that for all three turbulent wind components, using a 10 minute averaging period results in the largest values for maximum calculated power in the turbulent winds (given by the maximum power spectral density values), decreasing with decreasing averaging period. For example, for the longitudinal component the maximum value of the spectra is around 0.22 $(m/s)^2$/Hz for a 10 minute averaging period compared to almost 0.02 $(m/s)^2$/Hz for a 1 minute averaging period and maximum peaks are observed approximately at 0.008 Hz for 10 minutes averaging period but for 1 minute averaging period it moves to approximately 0.03 Hz. The trends in the spectral density curves for different averaging periods are, for each wind component, almost coincident but it is clear that more spectral frequencies have been collected during the longer averaging periods. In addition, the spectra of a longer data set exhibits more peaks over a wider range of frequencies especially in the starting part of the spectra. It is clear that averaging period affects the maximum value of the turbulence power spectra of wind in the built environment and different averaging periods will result in different power spectral density values. For the purpose of fatigue loads on a small wind turbine it would thus be important to investigate the power spectrum at least at 10 minutes averaging period to know what power is in the gusts that are hitting the blades of the turbine. In addition, using a longer averaging period will pick up more of the different frequencies (time-scales) of turbulence and this may be important in terms of resonance or noise in the interaction of the gust with the turbine blade. It is however, important to not choose an averaging period that is so long that it is outside the 'spectral gap' and the detail of the small-scale turbulence that impacts turbine blades is lost due to the mesoscale variations.

5. Conclusion

In this paper, the impact of sampling rate and averaging period on a turbulence study of the wind regime in the built environment is investigated. It is shown that choice of sampling rate does not significantly influence the values of turbulence intensity and power spectral density. In particular the characteristic turbulence intensity I_{15},a key parameter in the small wind standard IEC6400-2, does not appear to be sensitive to sampling rate. Changing the sampling rate from 10 Hz to 1 Hz changed the calculated value of I_{15} by at most 0.25%. Unlike sampling rate, changing the parameter of averaging period can significantly affect the results of calculated turbulence intensity, and value of I_{15}. A shorter averaging period results in a clear decrease in the recorded mean values of turbulence intensity for all wind components with a decrease in the value of I_{15} of approximately 17% in the case of reducing the averaging period from 10 minutes to 1 minute at z/h =1.70. Investigating the impact of averaging period on the turbulence power spectra shows that different averaging periods cause changes in the maximum turbulence power spectral density values. Generally, the results of this study show that the turbulence intensity and power spectra of the longitudinal and lateral components of wind over a rooftop are sensitive to choice of averaging period and because of this sensitivity, an averaging period of at least 10 minutes is suggested for rooftop wind monitoring to avoid underestimating values of turbulence intensity and turbulence power spectra.

Further, the results show that the required sampling rate and therefore type of anemometer used for a wind resource assessment in the built environment for the application of small wind turbines completely depends on the aim of the assessment. If the aim is just to investigate average turbulence intensity, I_{15}, and maximum longitudinal power spectral density values, 1 Hz sampling rate may provide results that are accurate enough. This is encouraging for more widespread monitoring of wind in the built environment as cup anemometers can sample at 1Hz and, despite price decreases in sonic anemometers in the last decade, are significantly cheaper than other options. Sampling at 1Hz, however, will not capture the full turbulence power spectra, in particular the very small-scale turbulence, and this may be a concern for an investigation that looks to predict the dynamic loading on a small wind turbine. In addition sampling at 1Hz may incorrectly predict the turbulence intensity and turbulence power spectra for the lateral and vertical components of wind fluctuations. Thus in the case where there is highly three-dimensional flow (a large lateral component of wind fluctuations due to e.g. extreme changes in wind direction, or a large vertical component of wind fluctuations due to e.g. vortex shedding) a sonic anemometer would be recommended. In summary, a 10Hz sampling rate and a 10 minute averaging period will give us upper estimates for values of turbulence intensity and turbulent power spectral density and this conservative approach may be best if we are looking to ensure that the wind resource assessment accurately captures the inflow to the wind turbine so that the turbine can be designed to handle both the loading and resonance due to turbulent gusting.

Acknowledgements

The authors would like to acknowledge Bunnings Group Pty. Ltd. for allowing Murdoch University researchers to conduct the wind monitoring campaign at the Port Kennedy warehouse. The authors are also indebted to Mr. Simon Glenister for maintaining the monitoring system and collecting data. Mr. Amir Bashirzadeh Tabrizi would like to thank Murdoch University for the award of a postgraduate scholarship. Dr. Jonathan Whale would like to thank the Hanse-Wissenschaftskolleg Institute of Advanced Study in Germany for the

award of a research fellowship that allowed him time to work on this research. Finally we thank our fellow members of the IEA Task 27 team for their support and enthusiasm for small wind turbine research.

References

[1] IEC 61400-2, Wind turbines-Part2: design requirements for small wind turbines, Second edition , International Electrotechnical Commission, Geneva, Switzerland, 2006.

[2] http://www.bergey.com/technical/warwick-trials-of-building-mounted-wind-turbines.

[3] http://www.cyclopicenergy.com/news/20100812-TurbineFailureHobart/Hobart-Marine-Board-Turbines.shtml.

[4] AWS Scientific, Inc. , Wind resource assessment handbook, National Renewable Energy Laboratory, Co, USA, 1997, Report No:SR-440-22223.

[5] IEC 61400-12, Wind turbine generator systems – Part 12: Wind turbine power performance testing, First edition, International Electrotechnical Commission, Geneva, Switzerland, 1998.

[6] S.J. Ross, M. P. McHenry, J. Whale, The impact of state feed in tariffs and federal tradable quota support policies on grid connected small wind turbine installed capacity in Australia, Renewable Energy, 46 (2012) 141-147.

[7] J. Whale, M.P. McHenry, A. Malla, Scheduling and conducting power performance testing of a small wind turbine, Renewable Energy, 55 (2013) 55-61.

[8] RenewableUK, Small and medium wind UK market report, April 2012.

[9] American wind energy association, 2011 U.S. small wind turbine market report, Year Ending 2011.

[10] A. Bashirzadeh Tabrizi, J. Whale, T. Lyons, T. Urmee, Performance and safety of rooftop wind turbines: use of CFD to gain insight into inflow conditions, *Renewable Energy*, 67 (2014), 242-251.

[11] A. Makkawi, A. Celik, T. Muneer, Evaluation of micro-mind turbine aerodynamics, wind speed sampling interval and its spatial variation, Services Engineering Research and Technology, 30 (2009) 7-14.

[12] V.A. Riziotis, S.G. Voutsinas, Fatigue loads on wind turbines of different control strategies operating in complex terrain, Wind Engineering and Industrial Aerodynamics, 85 (2000) 211-240.

[13] WINEUR, Report on Resource Assessment: WINEUR Deliverable 5.1, accessed February 2007, Online at http://www.urbanwind.org.

[14] D.C. Anderson, J. Whale, P.O. Livingston, D. Chan, Rooftop wind resource assessment using a Three-Dimension Ultrasonic Anemometer. In: 7th World Wind Energy Conference (WWEC2008), Kingston, Canada, June 24 – 26, 2008.

[15] M.W. Rotach, Profiles of turbulence statistics in and above an urban street canyon, Atmospheric Environment, 29 (1995) 1473-1486.

[16] L. Kristensen, Cup anemometer behavior in turbulent environments. Journal of Atmospheric and Oceanic Technology, 15 (1998) 5-17.

[17] S. Yahaya, J.P. Frangi, Cup anemometer response to the wind turbulence - measurement of the horizontal wind variance, Annales Geophysicae, 22 (2004) 3363-3374.

[18] V.R. Morris, J.C. Barnard, L.L. Wendell, S.D. Tomich, Comparison of anemometers for turbulence characterization, Windpower '92 Conference, Seattle, WA, USA,Oct 19-23,1992.

[19] T. S. Hristov, S. D. Miller, C.A. Friehe, Linear time-invariant compensation of cup anemometer and vane inertia, Boundary-Layer Meteorol, 97(2000) 293–307.

[20] F.C. Bosveld, A.C.M. Beljaars, The impact of sampling rate on eddy-covariance flux estimates, Agricultural and Forest Meteorology, 109 (2001) 39-45.

[21] W.D. Lubitz, Impact of ambient turbulence on performance of a small wind turbine, Renewable Energy, (2012) 1-5.

[22] S. Ruin, J. Whale, Consumer labelling for small wind turbines: Testing turbines in order to apply an international consumer label. Wind Tech International, 8 (2012) 24-27.

[23] I. Seginer, P. J. Mulhearn, E. F. Bradley, J. J. Finnigan, Turbulent flow in a model plant canopy, Boundary-Layer Meteorol , 10 (1976) 423-453.

[24] C. H. J. Stork, C. P. Butterfield, W. Holley, P. H. Madsen, P. H. Jensen, Wind conditions for wind turbine design proposals for revision of the IEC 1400-1 standard, Wind Engineering and Industrial Aerodynamics, 74-76 (1998) 443-454.

[25] J. L. Lumley, H. A. Panofsky, The structure of atmospheric turbulence, Interscience Publ., USA,1964.

[26] J. F. Manwell, J. G. McGowan, A. L. Rogers, Wind energy explained: theory, design and application, Second edition, John Wiley & Sons, Chichester , UK, 2009.

[27] R.B. Stull, An introduction to boundary layer meteorology, Kluwer Academic Publishers, Vancouver, Canada, 1988.

[28] T.J. Lyons, W. D. Scott, Principles of air pollution meteorology, Belhaven Press, London, 1990.

[29] U. Högström, A.S. Smedman, Kompendium i atmosfärens grässkikt. Del1. Turbulensteori och skikten närmast marken. Uppsala university, Uppsala, Sweden, 1989.

[30] D. Golder, Relations among stability parameters in the surface layer, Boundary Layer Meteorol. 3 (1972) 47-58.

[31] M. W. Rotach, Turbulence close to a rough urban surface. Part I: Reynolds Stress, Boundary Layer Meteorol. 65(1993) 1–28.

[32] M.S. Hossain, Investigating whether the turbulence model from existing small wind turbine standards is valid for rooftop sites, MSc Dissertation, School of Engineering and Energy, Murdoch University, Perth,Australia, 2012.

[33] I. Troen, E. L. Petersen, European Wind Atlas, Risø National Laboratory, Roskilde, Denmark, 1989.

[34] Small Wind Industry Implementation Strategy Consortium, Small wind turbine resource Assessment, 2005. URL http://www.smallwindindustry.org/index.php?id=122.

[35] www.warwickwindtrials.org.uk/resources/Warwick+Wind+Trials+Final+Report+.pdf.

[36] F. Fiedler and H. A. Panofsky, Atmospheric scales and spectral gaps, Bull. Amer. Meteor. Soc. 51(1970) 1114–1120.

[37] S. Lovejoy, D. Schertzer, and J. D. Stanway, Direct evidence of multifractal atmospheric cascades from planetary scales down to 1 km, Physical Review Letters, 86 (2001) 5200-5203.

[38] H.A. Panofsky, J.A. Dutton, Atmospheric turbulence, models and methods for engineering applications, John Wiley & Sons Inc., NY, 1984.

[39] K. Sunderland, T. Woolmington, J. Blackledge, M. Conlon, Small wind turbines in turbulent (urban) environments: A consideration of normal and Weibull distributions for power prediction, Wind Engineering and Industrial Aerodynamics, 121 (2013) 70-81.